ACETABULAR SHELL-LINER LOCKING MECHANISMS: INCFLIENCE ON BACKSIDE SLIDING RELATIVE MOTION AND BACKSIDE LINER DEFORMATION INTO SCREW HOLES

Timothy P. Harrigan*
Steven M. Kurtz*
Eric Charriere**
Robert M. Streicher**

Exponent, Inc., 2300 Chestnut St., Suite 150, Philadelphia, PA (*)
Stryker Europe, Clinical and Scientific Affairs, Thalwil, Switzerland (**)

INTRODUCTION

Clinical observation of focal lesions in the vicinity of screw holes or fenestrations in the metal shell has prompted researchers to suggest that backside wear or the fluidic pumping of polyethylene particles from other parts of the prosthesis may play an important role in the development of periprosthetic osteolysis. In addition, fluid pressure, even without particles, may also contribute to pelvic osteolysis. Cyclic fluid pressure with magnitudes of up to 0.138 MPa (20 psi) has been shown to activate macrophages, which play a major role in the onset of osteolysis at the implant/bone interface [1].

To assess these issues in a clinical situation, we developed contact-coupled finite element simulations of two commercially available acetabular components, based on the first and second generation of the ABG design (Stryker Howmedica Osteonics, Hérouville, France). These two generations of the ABG design differ primarily in the mechanism used to constrain the acetabular liner within the shell. In the ABG I, the liner is stabilized by two opposing extensions at the equator of the liner, which contact recesses in the outer shell, and by a conical extension at the pole of the liner which extends into a recess in the shell (figure 1). In the ABG II, the liner has 12 equally spaced extensions at the equator of the liner, which contact the outer shell, and it has no polar extension. The ABG I shell has 12 screw holes, spaced in two rows while the ABG II shell used in this study has five holes, concentrated in one area.

The purpose of this study was to assess the effect of changes in peripheral attachment on stresses and displacements at the liner-shell interface. We hypothesized that increased attachment at edge of this interface would significantly decrease liner/shell relative motion.

METHODS

Three dimensional finite element models were constructed of the ABG I and II designs based on the design drawings for a liner with a 32 mm inner diameter, a liner thickness of 5 mm, and a shell thickness of 4 mm, corresponding to a shell size of 50 mm. An additional set of models was constructed with a 28 mm head diameter, corresponding to a liner thickness of 7 mm. Thus, in addition to evaluating the effect of changes in shell and locking mechanism design, the femoral head diameter was also varied between 32 and 28 mm in this study. The inner radial clearance of the liner was 0.1 mm, and the outer radial clearance was 0.0 mm (perfectly conforming).

The finite element models approximated the interaction between the radial extensions of the liner and the outer shell by assuming that the outermost surface of the liner extension was fully bonded to a recess in the outer shell. Penalty-based contact was used between the prosthetic femoral head, the liner, and the outer shell was modeled with coulomb friction at the interfaces. The coefficient of friction was 0.085. The prosthetic femoral head and acetabular shell were modeled as rigid. The UHMWPE was modeled as elastic, (E= 974 MPa and ν=0.46). Data from Maxian et al. [2] was used to define 16 sequential quasistatic loading steps, coupled with flexion/extension of the femoral head, to describe the stance phase of a patient's gait cycle. The force-time history was linearly scaled such that the peak contact force during stance phase was 3,000 N. As in Maxian's analysis [2], the liner was assumed to be inclined at 45° from the horizontal.

The ABG I models used 37,696 eight-noded elements, with 44,768 nodes, and the ABG II models used 37,280 elements, with 44,357 nodes. The simulations used dynamic relaxation. Execution times on a 10-processor Linux Cluster, running LS-Dyna were 2.5 to 3.5 hours.

RESULTS

Stress and displacement results for the two designs, the two femoral head sizes, and the sixteen loading cycles were pooled to assess the influence of design, femoral head size, and loading condition on these variables. Table 1 shows the results of a statistical analysis of the data produced by the stress analyses. Changes in the design between the ABG I and II prostheses had a larger influence on the backside relative motion during the gait cycle than load magnitude. However, changes in the ABG I and II design had a smaller influence on the backside contact stress, von Mises stress, or radial extrusion into screw holes. Loading Magnitude had the largest influence on backside von Mises Stress, backside contact stress, and radial extrusion into screw holes.

The maximum radial extrusion into screw holes was 42 µm, and was found to be slightly lower for the ABG II when compared with the ABG I design throughout the stance phase of the gait cycle. Reduction in head size from 32 to 28 mm diameter resulted in a slight decrease in screw hole extrusion. An upper bound calculation was made for the fluid pressure increase due to extrusion of polyethylene into the screw hole, based on the change in the volume of fluid in the screw hole (from displacement data). Assuming no change in the fluid mass within the hole, the upper bound for fluid pressure was 10.7 MPa, which is orders of magnitude larger than pressures associated with osteolysis.

DISCUSSION

In this study, changes in the ABG design, including screw hole placement and increased peripheral interlocking, were shown to decrease relative motion at the liner-shell interface, but the peak liner-shell contact stresses, backside von Mises stresses, and radial screw hole extrusion were less significantly changed. The volume of fluid displaced by screw hole extrusion under load in these models is significant, and further study of the fluid flow within the screw holes should be undertaken.

REFERENCES

[1] Ferrier, *J Bone Joint Surg Br* 82, 2000 ;

[2] Maxian et al., *J. Biomechanics,* 29, 1996.

ACKNOWLEDGEMENT

Funded by a research grant from Stryker Europe.

Figure 1: ABG I Finite Element Model

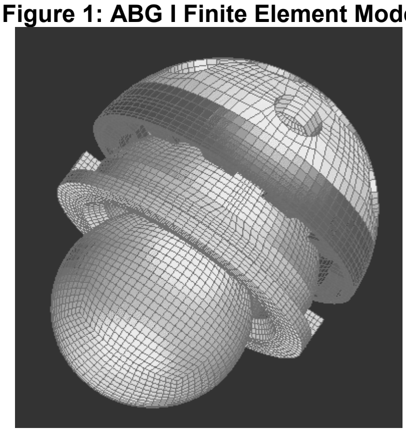

Table 1. Summary of r^2 values reflecting the variation in the backside sliding displacement, backside contact stress, backside von Mises stress, radial extrusion into screw holes which were accounted for by four independent model parameters. The r^2 values are calculated from the sum of the square d errors based on ANCOVA.

Independent Variable	Backside Sliding Motion	Backside Contact Stress	Backside von Mises Stress	**Extrusion into Screw Holes**
ABG I/II	0.458	0.000	0.074	0.034
Loading Type	0.039	0.005	0.006	0.000
Head Diameter	0.013	0.064	0.059	0.017
Load	0.224	0.871	0.781	0.914
Residual	0.266	0.060	0.079	0.035
Total	1.000	1.000	1.000	1.000